The 5th Joint International Conference on Multibody System Dynamics
June 24 – 28, 2018, Lisboa, Portugal

Study of contact descriptions in the framework of the absolute nodal coordinate formulation

Xinxin Yu[1], Ajay B. Harish[2], Marko K. Matikainen[1], Babak Bozorgmehri[1] and Aki Mikkola[1]

[1]*Mechanical Engineering, Lappeenranta University of Technology, marko.matikainen@lut.fi*
[2]*Institute of Continuum Mechanics, Leibniz Universität Hannover, harish@ikm.uni-hannover.de*

ABSTRACT — *Contact descriptions are often needed in applications of flexible multibody dynamics. There are different methods to determine body contacts, such as the time-stepping scheme including the linear complementarity problem (LCP), nonlinear complementarity problem (NCP), and penalty approaches. However, the contact description within multibody dynamics still remains a challenge, especially in the case of thousands or millions of contacts in the dynamic system or in the case of flexible bodies. This work demonstrates how contacts concerning a deformable body can be described using cone complementarity problems (CCP). In this study, a deformable body is modeled based on the absolute nodal coordinate formulation (ANCF) and it is combined with a friction/contact model based on CCP.*

1 Introduction

Multibody system dynamics is a general approach which can be used to describe equations of motion in a straightforward manner. The approach is utilized for a variety of applications, such as granular dynamics or mechanical systems consisting of rigid and flexible components. Contacts between rigid and/or flexible bodies exist in various multibody applications, such as belt drives, gears, bearings and human joints.

The absolute nodal coordinate formulation (ANCF) is a finite element based concept designed for usage with multibody system dynamics approach and can accurately predict the dynamic responses of two- and three-dimensional flexible bodies subjected to large deformations in multibody applications[1]. In this formulation, the nodal coordinates are defined using: (a) the absolute position vector (b) the slope vectors that can define the element orientation [2, 3]. A constant and symmetric mass matrix and highly nonlinear elastic forces from ANCF elements can provide some advantages during explict simulations [2].

Penalty method is often used to describe the contact between bodies and its implementation has been widely discussed. Some of the prominent works include those by Zavarise and Wriggers [4, 5] who have proposed both frictionless and frictional formulations for contact between circular beams in 3-D with the Coulomb friction model; Litewka and Wriggers [6] have analyzed a 3-D beam with rectangular cross-sections for frictional contacts; recently Durvile [7] has proposed the finite element approach to simulate the beam frictional contact interactions with large deformations. Durvile's study employs the detection of contact, which is defined from the proximity zone of between contact beams, such as self-contact beam. Wang et al. [8] has simulated frictional contacts of thin beam elements with the absolute nodal coordinate formulation (ANCF) where the minimal distance criterion is utilized to detect the contact. By employing the vector of nodal coordinates, the closest points from two contact beams can be defined in a straightforward manner.

The non-smooth nature of the non-penetration and the friction constraints during the contact [9] presents a significant numerical challenge and over the years plenty of novel numerical methods including several innovative time-stepping approaches have been proposed [10]. It is noteworthy to emphasize here that small time steps do not necessarily always ensure numerical stability in the case of multiple contacts. Therefore, researchers have proposed innovative time integration methods to solve this class of problems like the linear complementarity problem (LCP) and nonlinear complementarity problem (NCP) [11, 12]. The LCP method is frequently used to solve two-dimensional contact simulations by employing Lemke's algorithm. The NCP is recommended for use in the three-dimensional contact case [13]. However, when addressing a large number of contacts and polyhedral approximation used in friction [10], LCP and NCP solvers remain limited.

This work applies a contact description based on the cone complementarity problem (CCP) to the absolute nodal coordinate formulation. To this end, the paper introduces contact constraints and a friction model for the framework of the ANCF. Previously, the cone complementarity problem has been used to describe contacts in the case of rigid bodies only [14]. Accordingly, this paper introduces an important extension of the CCP approach. The remainder of this paper is organized as follows. Section 2 briefly introduces the methods and formulations, the beam element of the ANCF, definitions of the contact constraint, and the friction model. The section also explains the semi-implicit Euler method used to solve equations of motion including contacts. To validate the proposed approach, section 3 presents an example of element beam hitting the ground. followed by conclusions in Section 4.

2 Methods and formulations

2.1 Absolute nodal coordinate formulation

The ANCF beam element used in this study consists of three nodes, two of which are located at the end points and another at the midpoint of the beam axis. One position vector and one slope vector are included in the nodal coordinates. The position vector is denoted by $\boldsymbol{r}$ and the slope can be defined through the derivative of the displacement, which is $\boldsymbol{r}_{,y} = \frac{\partial \boldsymbol{r}}{\partial y}$. The vector of the nodal coordinates, $\boldsymbol{e}$ is

$$\boldsymbol{e} = \begin{bmatrix} \boldsymbol{r}^{(1)T} & \boldsymbol{r}_{,y}^{(1)T} & \boldsymbol{r}^{(2)T} & \boldsymbol{r}_{,y}^{(2)T} & \boldsymbol{r}^{(3)T} & \boldsymbol{r}_{,y}^{(3)T} \end{bmatrix}. \tag{1}$$

and as shown in Fig. 1.

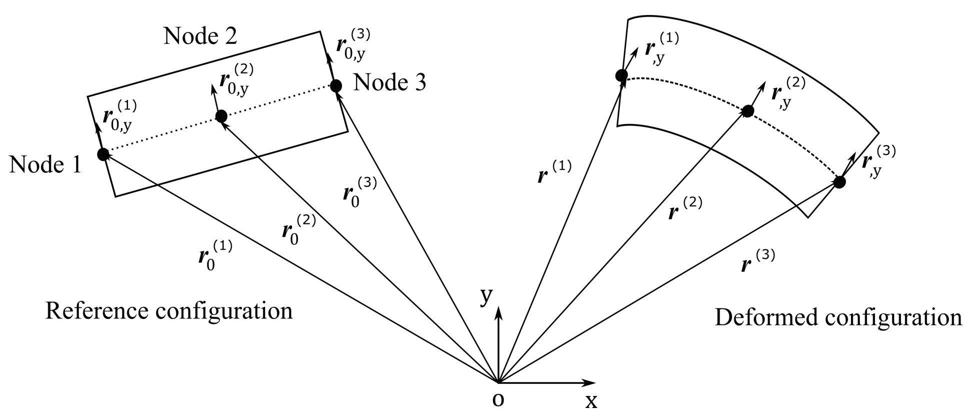

Fig. 1: Beam Kinematics defined in reference and deformed configuration

Each node has four degrees of freedom and thus this three-noded beam element has 12 degrees of freedom [15] whose shape functions can be defined in the bi-normalized local element coordinates (ξ,η) as:

$$S_1(\xi,\eta)=\frac{(\xi+1)^2}{2}-\frac{3\xi}{2}-\frac{1}{2} \qquad S_3(\xi,\eta)=2\xi-(\xi+1)^2+2 \tag{2a}$$

$$S_2(\xi,\eta)=\frac{\ell_y\eta}{2}+\frac{\ell_y\eta(\xi+1)^2}{4}-\frac{3\ell_y\eta(\xi+1)}{4} \qquad S_4(\xi,\eta)=\ell_y\eta(\xi+1)-\frac{\ell_y\eta(\xi+1)^2}{2} \tag{2b}$$

$$S_3(\xi,\eta)=2\xi-(\xi+1)^2+2 \qquad S_6(\xi,\eta)=\frac{\ell_y\eta(\xi+1)^2}{4}-\frac{\ell_y\eta(\xi+1)}{4} \tag{2c}$$

where the non-dimensional quantities $\boldsymbol{x}=(\xi,\eta)$ are defined as

$$\xi=\frac{x}{\ell_x},\eta=\frac{y}{\ell_y}, \tag{3}$$

where ℓ_x is the length of the beam element and ℓ_y is the height of the beam element in the undeformed configuration.

The shape function matrix for the beam element can be written with the help of Eq.(2c) in the following way:

$$\boldsymbol{S}_m=\begin{bmatrix}S_1\mathbf{I} & S_2\mathbf{I} & S_3\mathbf{I} & S_4\mathbf{I} & S_5\mathbf{I} & S_6\mathbf{I}\end{bmatrix}, \tag{4}$$

where $\mathbf{I}$ is the 2-by-2 identity matrix.

Using the ANCF formulation, any arbitrary particle of the element can be defined with respect to the global coordinates, the shape function Eq.(4), and the vector of nodal coordinates Eq.(1) as

$$\boldsymbol{r}=\boldsymbol{S}_m\boldsymbol{e}. \tag{5}$$

The mass matrix of the element can be obtained with the help of kinetic energy

$$T=\frac{1}{2}\int_V\rho\dot{\boldsymbol{r}}^T\dot{\boldsymbol{r}}\,\mathrm{d}V, \tag{6}$$

where $\dot{\boldsymbol{r}}=\frac{d\boldsymbol{r}}{dt}$ is the time derivative of $\boldsymbol{r}$ given by Eq.(5), ρ is mass density, and V is the volume of the beam finite element. The velocity of a particle $\dot{\boldsymbol{r}}$ can be written as:

$$\dot{\boldsymbol{r}}=\boldsymbol{S}_m\dot{\boldsymbol{e}}. \tag{7}$$

Substituting Eq.(7) into Eq.(6), the kinetic energy can be written as

$$T=\frac{1}{2}\dot{\boldsymbol{e}}^T\left[\int_V\rho\boldsymbol{S}_m^T\boldsymbol{S}_m\,dV\right]\dot{\boldsymbol{e}}=\frac{1}{2}\dot{\boldsymbol{e}}^T\boldsymbol{M}\dot{\boldsymbol{e}}, \tag{8}$$

where $\boldsymbol{M}$ is the mass matrix.

2.2 Non-penetration contact constraints and friction model

Contact points can be defined by employing the global nodal coordinates of the beam elements of the ANCF. As Fig. 2 shows, many contact points can be defined from both element A and element B. The closest arbitrary contact points P_A and P_B of two elements, can be adopted to determine if the two elements come into contact. Here, the distance of the closest contact points is defined as gap function Φ_i. When the contact takes a place, the beam should not penetrate, which means the gap function Φ_i that is closer than a prescribed distance can be defined to produce a contact event.

Φ_i can be expressed as

$$\Phi_i = \|\boldsymbol{r}_A^{P_A} - \boldsymbol{r}_B^{P_B}\|, \tag{9}$$

where $\boldsymbol{r}_A^{P_A}$ and $\boldsymbol{r}_B^{P_B}$ are the contact points associated with element A and element B,respectively. These position vectors can be calculated using Eq.(5). The non-penetration constraints can be expressed as

$$\Phi_i \geq 0, \tag{10}$$

where i represents the i-th contact.

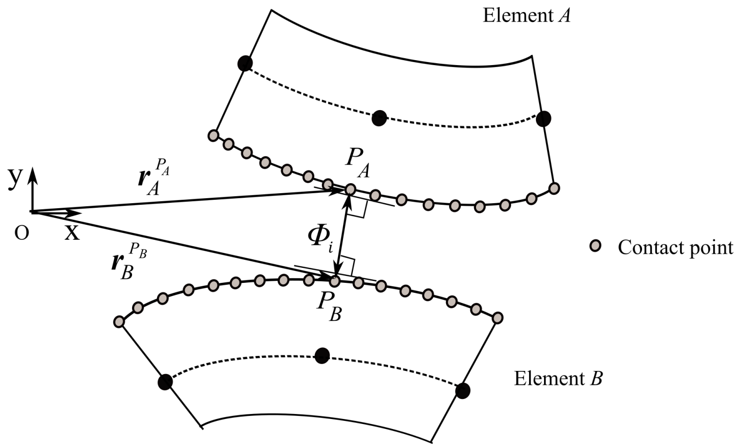

Fig. 2: Element contact detection

In this work, the Coulomb friction law is adopted as the relation between the normal and tangential force at the contact point. When the system is governed by normal contact force $\boldsymbol{f}_2$ and the tangential contact force $\boldsymbol{f}_1$, which is perpendicular to $\boldsymbol{f}_2$, the relation between the two contact forces can be defined as:

$$\boldsymbol{f}_2 \geq 0, \tag{11a}$$

$$\mu \boldsymbol{f}_2 - \boldsymbol{f}_1 \geq 0, \tag{11b}$$

where $\mu \geq 0$ is the coefficient of friction with a value between 0 and 1.

2.3 Equation of motion

For contact event i, a collision detection process produces the point of contact P, a signed distance function Φ_i, and a set of two orthonormal vectors $\boldsymbol{n}_i$ and $\boldsymbol{\tau}_i$ at the contact plane, as defined in Fig. 3. The vector $\boldsymbol{n}_i$ is normal with respect to the contact point, which leads from element A to the ground, and the vector $\boldsymbol{\tau}_i$ is tangential with respect to the contact point.

If the contact is active, then $\Phi_i^P = 0$. So, at the contact point, the force acting on element A at point P is as follows:

$$\boldsymbol{F}_i = \boldsymbol{\tau}_i \hat{\gamma}_{i,\tau} + \boldsymbol{n}_i \hat{\gamma}_{i,n} = \begin{bmatrix} \boldsymbol{\tau}_i & \boldsymbol{n}_i \end{bmatrix} \begin{bmatrix} \hat{\gamma}_{i,\tau} \\ \hat{\gamma}_{i,n} \end{bmatrix} = \boldsymbol{A}_i \hat{\gamma}_i, \tag{12}$$

where $\boldsymbol{A}_i = \begin{bmatrix} \boldsymbol{\tau}_i & \boldsymbol{n}_i \end{bmatrix}$ is the orthogonal rotation matrix consisting of unit orthogonal tangential and normal vectors at the i-th contact point. The contact force is imposed on the system by means of multipliers $\hat{\gamma}_{i,\tau}$ and $\hat{\gamma}_{i,n}$; that

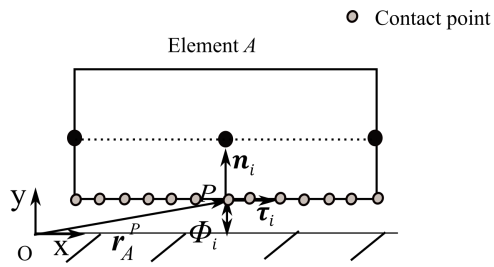

Fig. 3: Illustration of element A contact with the ground

is, the tangential component of the force is $\boldsymbol{f}_1 = \boldsymbol{\tau}_i \hat{\gamma}_{i,\tau}$ and the normal component of the force is $\boldsymbol{f}_2 = \boldsymbol{n}_i \hat{\gamma}_{i,n}$. So, $\hat{\gamma}_i = \begin{bmatrix} \hat{\gamma}_{i,\tau} \\ \hat{\gamma}_{i,n} \end{bmatrix}$.

Assume that there are N_K potential contacts, so that the contact constraints are enforced by non-penetration constraints $\Phi_i > 0, i = 1,2,....$ Here, superscript i is the frequency of the potential contact. The contact matrix can be constructed as

$$\hat{\gamma} = \begin{bmatrix} \hat{\gamma}_1 & \dots & \hat{\gamma}_{N_K} \end{bmatrix}. \tag{13}$$

Different forces act in the system when the beam element comes into contact, including the external force $\boldsymbol{F}_{exter}$, the elastic force $\boldsymbol{F}_{elast}$ and the frictional contact force $\boldsymbol{D}\hat{\gamma}$. Therefore, the equation of motion takes the form

$$\boldsymbol{M}\ddot{\boldsymbol{e}} = \boldsymbol{F}_{exter} - \boldsymbol{F}_{elast} + \boldsymbol{D}\hat{\gamma}, \tag{14}$$

where matrix $\boldsymbol{D}$ is the contact transformation matrix, which can convert the general force to contact force. According to Eq.(14), the equations of motion can be expressed as ~~follows:~~

$$\boldsymbol{M}\frac{\left(\dot{\boldsymbol{e}}^{(l+1)} - \dot{\boldsymbol{e}}^{(l)}\right)}{\Delta t} = \boldsymbol{F}_{exter}^{(l)} - \boldsymbol{F}_{elast}^{(l)} + \boldsymbol{D}^{(l)}\hat{\gamma}^{(l+1)}, \tag{15}$$

where $\dot{\boldsymbol{e}}^{(l)}$ is the general known velocity and $\dot{\boldsymbol{e}}^{(l+1)}$ is the unknown velocity with time step Δt.

The external force $\boldsymbol{F}_{exter}$ can be calculated from the external virtual work δW_{exter} as ~~follows:~~

$$\delta W_{exter} = \int_V \boldsymbol{b}^T \delta\boldsymbol{r}\, \mathrm{d}V. \tag{16}$$

Eq.(5) gives the virtual displacement, that is:

$$\delta\boldsymbol{r} = \frac{\partial\boldsymbol{r}}{\partial\boldsymbol{e}}\delta\boldsymbol{e} = \boldsymbol{S}_m\delta\boldsymbol{e}, \tag{17}$$

therefore, Eq.(16) can be transformed to

$$\delta W_{exter} = \int_V \boldsymbol{b}^T \boldsymbol{S}_m\, \mathrm{d}V\, \delta\boldsymbol{e}, \tag{18}$$

where $\boldsymbol{b}$ is the vector of the body forces. In this case, the body force is the gravity force, which can be written as $\boldsymbol{b} = \rho\boldsymbol{g}$, where $\boldsymbol{g}$ is the field of gravity.

From Eq.(18), the external force $\boldsymbol{F}_{exter}$ can be identified as~~:~~

$$\boldsymbol{F}_{exter} = \int_V \boldsymbol{b}^T \boldsymbol{S}_m\, \mathrm{d}V. \tag{19}$$

The elastic force $\boldsymbol{F}_{elast}$, in turn, can be derived from the virtual work of elastic forces δW_{elast},

$$\delta W_{elast} = \int_V \boldsymbol{S} : \delta \boldsymbol{E} \, \mathrm{d}V = \int_V \boldsymbol{S} : \frac{\partial \boldsymbol{E}}{\partial \boldsymbol{e}} \, \mathrm{d}V \, \delta \boldsymbol{e}, \tag{20}$$

in which : denotes the double dot product, $\boldsymbol{S}$ is the second Piola-Kirchhoff stress tensor and $\boldsymbol{E}$ is the Green strain tensor.~~The Green strain tensor can be~~ written as

$$\boldsymbol{E} = \frac{1}{2}(\boldsymbol{F}^T \boldsymbol{F} - \mathbf{I}), \tag{21}$$

where $\mathbf{I}$ is the identity tensor and $\boldsymbol{F}$ is the deformation gradient tensor, which is

$$\boldsymbol{F} = \frac{\partial \boldsymbol{r}}{\partial \boldsymbol{r}_0} = \frac{\partial \boldsymbol{r}}{\partial \boldsymbol{x}} \frac{\partial \boldsymbol{x}}{\partial \boldsymbol{r}_0} = \begin{bmatrix} \frac{\partial r^{(1)}}{\partial \xi} & \frac{\partial r^{(1)}}{\partial \eta} \\ \frac{\partial r^{(2)}}{\partial \xi} & \frac{\partial r^{(2)}}{\partial \eta} \\ \frac{\partial r^{(3)}}{\partial \xi} & \frac{\partial r^{(3)}}{\partial \eta} \end{bmatrix} \begin{bmatrix} \frac{\partial r_0^{(1)}}{\partial \xi} & \frac{\partial r_0^{(1)}}{\partial \eta} \\ \frac{\partial r_0^{(2)}}{\partial \xi} & \frac{\partial r_0^{(2)}}{\partial \eta} \\ \frac{\partial r_0^{(3)}}{\partial \xi} & \frac{\partial r_0^{(3)}}{\partial \eta} \end{bmatrix}^{-1}, \tag{22}$$

where $\boldsymbol{r}$ and $\boldsymbol{r}_0$ are the current and initial configuration, respectively.

2.4 Reformulation as the cone complementarity problem

The cone complementarity problem (CCP) represents the first order optimality conditions for the convex quadratic optimization problem with conic constraints:

$$\begin{aligned} \gamma^{(l+1)} =& \min \frac{1}{2} \gamma^T \boldsymbol{N} \gamma + \boldsymbol{p}^T \gamma, \\ & \text{subject to } \gamma_i \in \mathbb{C}_i \end{aligned} \tag{23}$$

where $\gamma = \hat{\gamma} \Delta t$ is the contact impulse when the element is experiencing contact and $\gamma^{(l+1)}$ is the unknown contact impulse at the next time step Δt. $\mathbb{C}_i$ is from the Coulomb friction model in Eq.(11). In Eq.(23), $\boldsymbol{N}$ is the Hessian matrix of the objective function containing all of the (twice-differentiated) quadratic terms, and $\boldsymbol{p}$ is the Hessian matrix's gradient containing all of the (simply-differentiated) linear terms.

According the CCP optimization method of Eq.(23), matrix $\boldsymbol{N}$ can be defined as follows:

$$\boldsymbol{N} = \boldsymbol{D}^T \boldsymbol{M}^{-1} \boldsymbol{D}. \tag{24}$$

Correspondingly, the matrix $\boldsymbol{p}$ can be defined as follows:

$$\boldsymbol{p} = \boldsymbol{d}_{i,0} + \boldsymbol{D}^{(l),T} \left(\dot{\boldsymbol{e}}^{(l)} + \boldsymbol{M}^{-1} \boldsymbol{F}_{exter}^{(l)} \Delta t - \boldsymbol{M}^{-1} \boldsymbol{F}_{elast}^{(l)} \Delta t \right), \tag{25}$$

where the term of $\boldsymbol{d}_i$ is

$$\boldsymbol{d}_{i,0} = \begin{bmatrix} 0 \\ \frac{1}{\Delta t} \boldsymbol{\Phi}_i^{(l)} \end{bmatrix}. \tag{26}$$

2.5 Discretized equations with semi-implicit Euler method

Using a semi-implicit Euler numerical scheme for Eq.(15) at time step $t^{(l+1)} = t^{(l)} + \Delta t$, the velocity within time step $\dot{\boldsymbol{e}}^{(l+1)}$ can be calculated as

$$\dot{\boldsymbol{e}}^{(l+1)} = \dot{\boldsymbol{e}}^{(l)} + (\boldsymbol{M}^{-1}\boldsymbol{F}^{(l)}_{exter} - \boldsymbol{M}^{-1}\boldsymbol{F}^{(l)}_{elast} + \boldsymbol{M}^{-1}\boldsymbol{D}^{(l)}\hat{\gamma}^{(l+1)})\Delta t. \tag{27}$$

The generalized position of the element can be calculated as

$$\boldsymbol{e}^{(l+1)} = \boldsymbol{e}^{(l)} + \dot{\boldsymbol{e}}^{(l+1)}\Delta t. \tag{28}$$

With time integration, the new contact impulse $\gamma^{(l+1)}$ will be computed using Eq.(23). The new velocity $\dot{\boldsymbol{e}}^{(l+1)}$ can be obtained via Eq.(27). The new position $\boldsymbol{e}^{(l+1)}$ will finally be calculated through Eq.(28).

3 Numerical example

A beam element coming into contact with the ground is studied as an numerical example. The dimensions of the beam are assumed as $H = 0.1$ m and $L = 1$ m. The density is $\rho = 7850$ kg/m^3 and Young's modulus is $E = 2.1 \times 10^8$ N/m^2. The Poisson's ratio of the beam material is $\nu = 0.3$. The Lamé constants are $\lambda = E\nu/[(1+\nu)(1-2\nu)]$ and $\mu = E/[2(1+\nu)]$. The time step is $\Delta t = 0.0001$ s and the final time is $t = 2.5$ s.

The beam is freefalling from the height of $h = 5$m with zero initial velocity. The gravity force makes the beam move vertically, hit the ground, bounce up and then hit the ground again. Fig. 4 and Fig. 5 show the dynamic configurations of the system at the first and second contacts. As the figures show, the beam will deform after its contact with the ground.

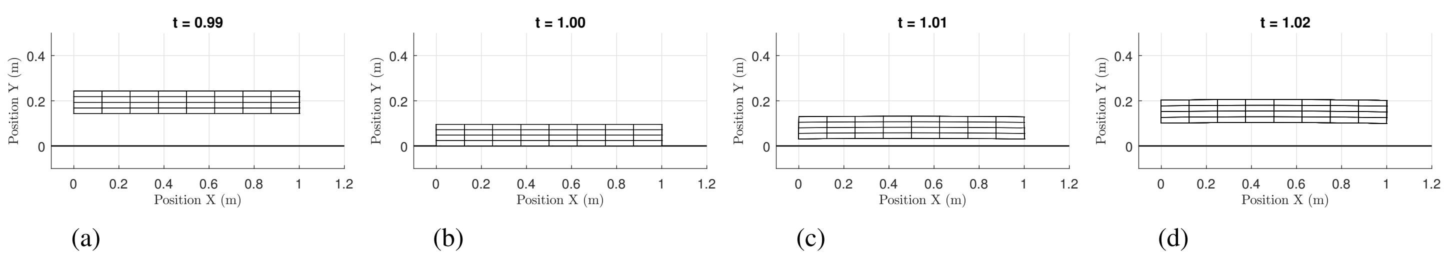

Fig. 4: Illustration of the shape of the beam during the first contact visualized by Matlab

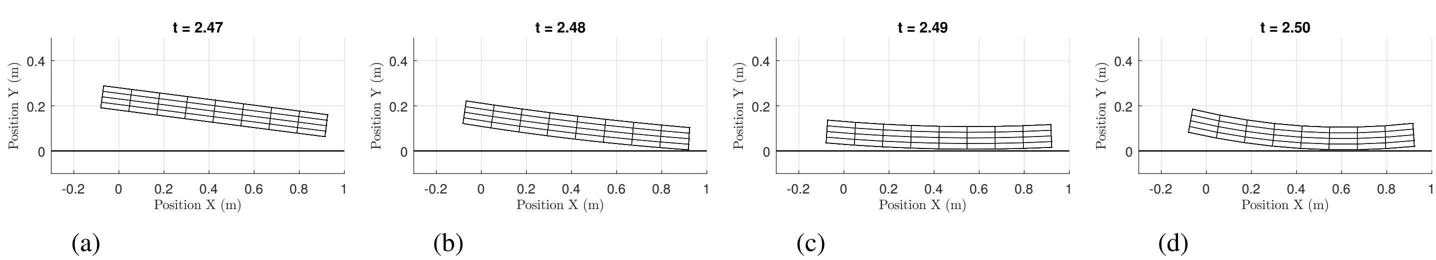

Fig. 5: Illustration of the shape of the beam during the second contact visualized by Matlab

Fig. 6 shows the vertical displacement of the beam with the time.

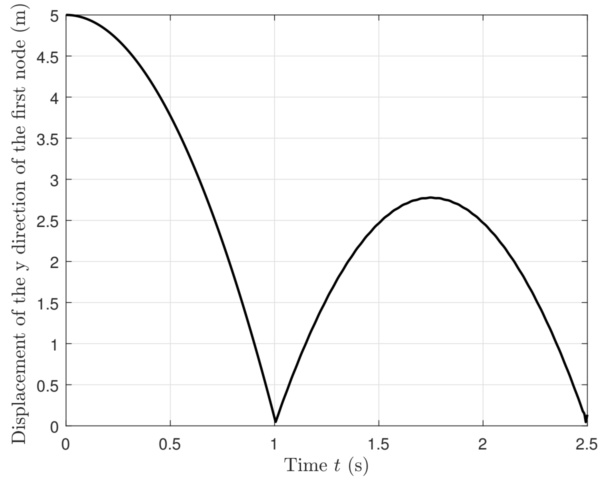

Fig. 6: The displacement of the y direction of the first node of the element

4 Conclusions

Contact problems have received extensive attention in multibody applications due to their importance in engineering. This paper reports the derivation and the numerical simulation of a flexible beam element's contact dynamic problems based on the ANCF. The novelty of this work is the combination with the friction/contact model based on the CCP. The ANCF approach and CCP method are explained in detail. The one element beam hitting the ground is studied as a numerical example. The numerical example suggests that the CCP method used in the flexible beam can work well.

The next step in the development will be the inclusion of the beam to beam contact. The 3-D contact case will also be analyzed in the future. This will require some additional constraint definitions. Furthermore, the work can be combined with the implicit time-stepping method to make the simulation more precise and efficient.

References

[1] A. A. Shabana, "Flexible multibody dynamics: review of past and recent developments," *Numerische Mathematik*, vol. 68, no. 1, pp. 95–106, 1994.

[2] M. Berzeri, M. Campanelli, and A. A. Shabana, "Definition of the elastic forces in the finite element absolute nodal coordinate formulation and the floating frame of reference formulation," *Multibody System Dynamics*, vol. 5, no. 1, pp. 21–54, 2001.

[3] A. A. Shabana, "Definition of the slopes and the finite element absolute nodal coordinate formulation," *Multibody System Dynamics*, vol. 1, no. 3, pp. 339–348, 1997.

[4] P. Wriggers and G. Zavarise, "On contact between three-dimensional beams undergoing large deflections," *Communications in Numerical Methods in Engineerings*, vol. 13, no. 6, pp. 429–438, 1997.

[5] G. Zavarisel and P. Wriggers, "Contact with friction between beams in 3-D space," *International Journal for Numerical Methods in Engineering*, vol. 49, no. 8, pp. 977–1006, 2000.

[6] P. Litewka and P. Wriggers, "Frictional contact between 3-D beams," *Computational Mechanics*, vol. 28, no. 1, pp. 26–39, 2002.

[7] D. Durvile, "Contact friction modeling within elastic beam assemblies: an application to knot tightening," *Computational Mechanics*, vol. 49, no. 6, pp. 687–707, 2012.

[8] Q. Wang, Q. Tian, and H. Hu, "Dynamic simulation of frictional contacts of thin beams during large overall motions via absolute nodal coordinate formulation," *Nonlinear Dynamics*, vol. 77, no. 4, pp. 1411–1425, 2014.

[9] T. F. Pfeiffer and C. Glocke, *Multibody dynamics with unilateral contacts*. New York: Wiley Series in Nonlinear Science, 1996.

[10] M. Anitescu and A. Tasora, “An iterative approach for cone complementarity problems for nonsmooth dynamics,” *Computational Optimization and Applications*, vol. 47, no. 2, pp. 207–235, 2010.

[11] Kočvara and J. Zowe, “An iterative two-step algorithm for linear complementarity problems,” *Numerische Mathematik*, vol. 68, no. 1, pp. 95–106, 2008.

[12] W.-L. Yao, B. Chen, C.-S. Liu, and J. Xu, “Dynamics of multi-rigid-body systems under non-smooth constraints and linear complementary problems,” *International Journal of Computer Mathematics*, vol. 85, no. 6, pp. 889–898, 2008.

[13] M. J. Mashayekhi and J. Kovecses, “A comparative study between the augmented lagrangian method and the complementarity approach for modeling the contact problem,” *Multibody System Dynamics*, vol. 40, no. 4, pp. 327–345, 2017.

[14] A. Tasora and M. Anitescu, “A fast NCP solver for large rigid-body problems with contacts, friction, and joints,” in *Multibody Dynamics: Computational Methods and Applications*, pp. 45–55, Springer, Berlin 2008.

[15] K. Nachbagauer, P. Gruber, and J. Gerstmayr, “A 3-D shear deformable finite element based on the absolute nodal coordinate formulation,” *Multibody Dynamics: Computational Methods in Applied Sciences*, vol. 28, pp. 77–96, 2013.